

Casting effect on compressive brittleness of bulk metallic glass

Hong WU^{1,2}, Yong LIU¹, Kai-yang LI¹, Zhong-wei ZHAO²

1. State Key Laboratory of Powder Metallurgy, Central South University, Changsha 410083, China;
2. School of Metallurgy and Environment, Central South University, Changsha 410083, China

Received 5 March 2013; accepted 28 October 2013

Abstract: An interesting phenomenon of cooling-rate induced brittleness in $Zr_{52.5}Cu_{17.9}Ni_{14.6}Al_{10}Ti_5$ bulk metallic glass (BMG) was reported. It was found that the as-cast BMG specimens exhibited a brittle–ductile transition when the larger specimens were machined into smaller specimens through removing the cast-softening surface layer by layer. After compression tests, the as-machined small specimens, owing to the absence of the cast-softening surface, displayed highly dense and intersecting shear bands, and extensive plastic deformation. This is in contrast to the catastrophic failure and low deformability in the as-cast large specimens. More free volume was detected in the smaller as-fractured specimens, by differential scanning calorimetry, which may be attributed to the occurrence of strain softening and increased plasticity. Compared with the relatively smooth fracture surface in the smaller specimens, the larger specimens showed more diverse features on the fracture surface due to their graded structures.

Key words: bulk metallic glasses; mechanical behavior; plastic deformation; shear band; free volume

1 Introduction

Bulk metallic glasses (BMGs) have aroused extensive interest because of their superior mechanical properties, such as ultra-high strength, large elastic limit and high hardness [1,2]. Metallic glasses, however, are also known for extremely brittle behavior, failing in a catastrophic fracture manner, as a result of the formation of highly localized shear bands, which greatly limits their engineering applications [3]. In recent years, increasing efforts have been made to improve the plasticity of BMGs, such as the inclusion of micrometer- or nanometer-sized structural heterogeneities [4,5], nanometer-scale phase separation [6], the addition of minor elements [7], and the optimization of Poisson ratio [8]. In addition to these methods that control the intrinsic composition and microstructure of the metallic glasses, recent studies show that several physical approaches can dramatically enhance the deformability of BMGs, such as shot peening [9], surface roughness [10], surface severe plastic deformation process [11], and pre-straining process [12].

Over the past decades, cooling-rate effects on the

mechanical behaviors have been widely investigated in many kinds of materials, such as steels [13], polymers [14], and various metallic alloys [15]. In crystalline metals, their mechanical performance was significantly improved due to the formation of the high strength and toughness phase through a high cooling rate process [13]. Nevertheless, although most metallic glasses only have monolithic amorphous phase without long-ordered atomic arrangement, in the last few years, casting effects, induced by the variation of cooling rate during the fabrication process, have also been reported in many metallic glass systems [16–19]. It is generally considered that the free volume plays an important role in interpreting the plastic flow of metallic glasses [20,21]. Recent studies indicate that a large amount of free volume produced by a fast cooling rate of an amorphous matrix leads to low hardness [16] but improves macroscopic plasticity [17]. Microscopically, cooling-rate difference during casting induced surface softening was reported in different metallic glasses, which is presumably ascribed to the variation of defect concentration (free volume) [18,19]. To our knowledge, the testing BMG samples were generally viewed as a thoroughly uniform and homogeneous entity, while the

Foundation item: Project (2012M511401) supported by China Postdoctoral Science Foundation; Project (12JJ5018) supported by Hunan Provincial Natural Science Foundation of China; Project (2012RS4006) supported by Hunan Provincial Science and Technology Plan of China; Project (CSUZC2012028) supported by the Open-End Fund for the Valuable and Precision Instruments of Central South University, China

Corresponding author: Yong LIU; Tel: +86-731-88830406; E-mail: yonliu11@yahoo.com.cn
DOI: 10.1016/S1003-6326(14)63073-9

effects of such casting induced surface softening on the macroscopic mechanical behavior of BMGs have not been investigated. Further, the surface conditions impacting the macroscopic deformability of BMGs are commonly recognized [9–11]. Similarly, can the cast-softened surface affect the macroscopic mechanical behavior of BMGs? How does it behave during and after deformation? These are questions we intend to address here.

In the present study, the effects of casting induced surface softening on compressive behavior of a Zr-based BMG were investigated through removing the cast-softened surface layer by layer. The underlying mechanisms of these effects and related fracture behavior were discussed.

2 Experimental

A Zr-based BMG, $Zr_{52.5}Cu_{17.9}Ni_{14.6}Al_{10}Ti_5$, was chosen for this study because of its good glass forming ability, which allowed casting metallic glass specimens with 6.7 mm in diameter [22]. The master alloy was prepared by arc melting a mixture of Zr (99.8%), Cu (99.9%), Ni (99.9%), Al (99.99%), and Ti (99.9%) in a Ti-gettered high-purity argon atmosphere. The ingot was remelted four times to ensure a homogeneous composition, and then was suction cast into a 5 mm diameter and 70 mm length, in water-cooled copper mold. The amorphous nature of the material was confirmed with a Rigaku-3014 X-ray diffractometer (XRD) using Cu K_α radiation. The thermodynamic behavior of the specimens was investigated using an SDT Q600 differential scanning calorimeter (DSC), from room temperature to 1000 K at a heating rate of 20 K/min under flowing argon.

Part of the as-cast glassy rods were machined into cylindrical specimens with either 3 mm or 1.2 mm in diameter. All the specimens, including 5 mm diameter as-cast specimens, were hand-polished with a 15 μm emery paper; the ends were polished by mounting in a mold to ensure that both end surfaces were aligned perpendicular to the loading axis. All the specimens had a height to diameter ratio of 2:1. Compression tests were carried out using a CSS-44100 testing machine at an initial strain rate of $3 \times 10^{-4} \text{ s}^{-1}$ at room temperature. Specimens of the same size were tested at least three times. Following the compression tests, the fracture surface morphology and the vertical sides of the specimen were examined using a Sirion-100 scanning electron microscope (SEM). The microstructures of the as-deformed samples were determined using an FEI Tecnai F20 field emission gun transmission electron microscope (FEG-TEM). The Vickers microhardness was measured using a Leitz Miniload microhardness

tester at a load of 50 g (0.49 N).

3 Results

3.1 Mechanical behavior

XRD patterns of the as-cast (5 mm) and as-machined (3 mm and 1.2 mm) specimens are shown in Fig. 1. There are typical patterns of amorphous structures with only a broad diffraction halo, and no detectable sharp Bragg peaks corresponding to crystalline phases. Figure 2 shows the compressive engineering strain–stress curves for specimens with three different diameters. For each specimen, the strain–stress curve is linear up to about 2% elastic strain, after which yielding and plastic deformation occur. The strain to failure was found to increase significantly as the specimen size decreased. Table 1 shows the mechanical properties of the specimens with different diameters, including the yield strength σ_y , the fracture strength σ_f , and the plastic strain to failure ϵ_p . Accordingly, the

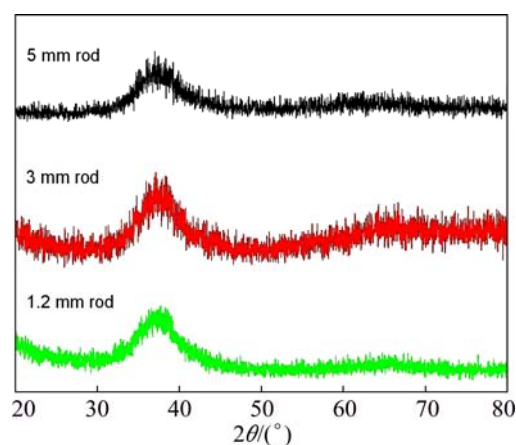


Fig. 1 XRD patterns of as-cast (5 mm) and as-machined (3 mm and 1.2 mm) $Zr_{52.5}Cu_{17.9}Ni_{14.6}Al_{10}Ti_5$ alloy rods

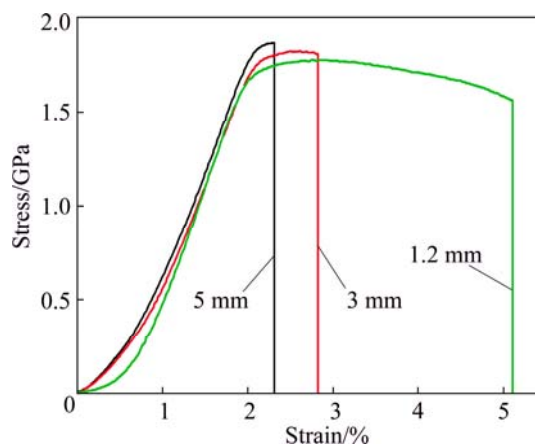


Fig. 2 Compressive engineering strain–stress curves of $Zr_{52.5}Cu_{17.9}Ni_{14.6}Al_{10}Ti_5$ glassy rods with different specimen sizes at room temperature (The results with the maximum plasticity of each specimen size are shown in the graph)

Table 1 Mechanical and thermal properties of glassy rods with different specimen size

$D/$ mm	$\sigma_y/$ MPa	$\sigma_f/$ MPa	$\varepsilon_p/$ %	$T_g/$ K	$T_x/$ K	$\Delta H_{sr}/$ ($J \cdot g^{-1}$)
5	1753±12	1858±12	0.17±0.13	678	727	0.6
3	1697±15	1812±13	0.42±0.38	676	725	1.3
1.2	1626±12	1763±13	2.21±0.89	672	722	3.2

D —Specimen diameter; σ_y —Yield strength; σ_f —Fracture strength; ε_p —Plastic strain; T_g —Glass transition temperature; T_x —Crystallization temperature; ΔH_{sr} —Structural relaxation exothermic heat

specimen size has an impact on the plasticity. The yield strength and fracture strength of the specimens decrease with the specimen size.

3.2 Morphology and microstructure

Due to the absence of lattice order, the ductility of metallic glasses is governed by the cumulative behavior of shear band development rather than multiplication and movement of dislocations. The latter is the case for crystalline metals. To understand the possible reasons for such size-dependant mechanical behavior, the vertical sides of the fractured specimens were examined. Figure 3 shows SEM images of the side surfaces of the fractured specimens with diameters of 5 mm and 1.2 mm at different magnifications. The number of visible shear bands in the specimen with 5 mm in diameter appears to be markedly less than that observed for the 1.2 mm

specimen. Only sparse, scattered shear bands were observed on the side surface of the 5 mm specimen, as shown in Figs. 3(a) and (c). In contrast, dense and multiple shear bands are visible on the whole side surface of 1.2 mm specimen, as shown in Figs. 3(b) and (d). The shear bands are homogeneously distributed, indicating that there is no significant localization of the shear bands. The dense, frequently branching and numerous intersections of shear bands may be the reason for the enhanced plasticity. As for the orientation of the fracture surface, all the samples of different diameters fractured at approximately 45° to the compression axis, which is consistent with the typical shear–fracture modes reported in the literatures for the same BMG [22–24].

The plasticity of BMGs can be enhanced due to the presence of micrometer-sized crystallinities and nanometer-sized crystallinities, which are usually introduced into BMGs to form composites [5]. Crystallization and nanocrystallization of BMGs caused by deformation have been reported in previous studies [3]. However, the XRD results obtained from a more heavily deformed specimen ($\varepsilon_p=80\%$) of the same composition BMG revealed no evidence of crystallization [23]. To further confirm the amorphous nature of as-deformed samples, TEM analyses were performed. A bright-field TEM image of 1.2 mm deformed sample is shown in Fig. 4. A uniform

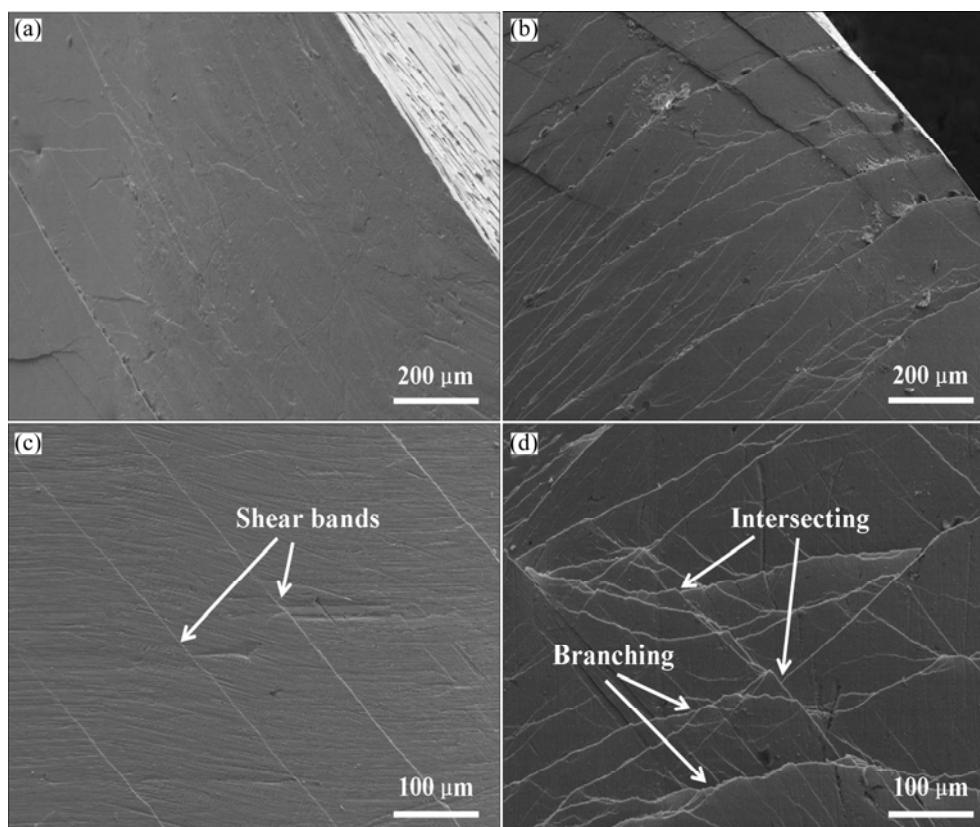


Fig. 3 SEM images of side surface of fractured specimens with diameters of 5 mm (a, c) and 1.2 mm (b, d)

microstructure with no contrasting phases was confirmed. Besides, the corresponding selected-area diffraction (SAD) pattern shows an amorphous ring (the inset of Fig. 4), also indicating its nearly fully amorphous structure.

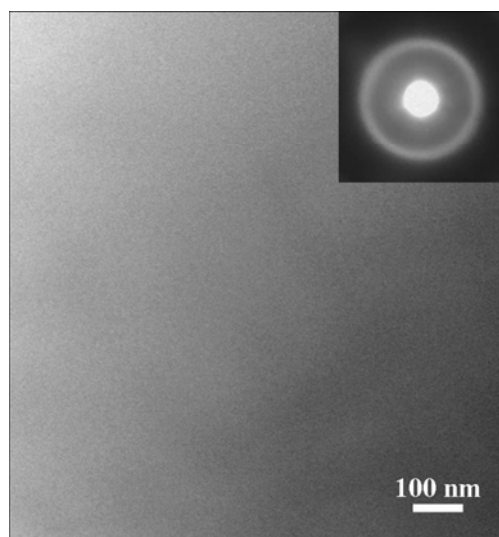


Fig. 4 Bright-field TEM image of 1.2 mm deformed specimen and corresponding selected-area diffraction pattern

3.3 Thermal analysis

In order to further explore the underlying mechanisms for the size-dependant mechanical behavior, the thermal properties of the glassy specimens were measured. Figure 5(a) presents DSC curves of the as-fractured specimens with different diameters at a heating rate of 20 K/min. The DSC curves of un-deformed specimens measured under the same conditions are shown in Fig. 5(b) for comparison. All of the specimens exhibit a clear glass transition and a wide supercooled liquid region, followed by a couple of exothermic reactions associated with crystallization processes. A slight decrease in the glass transition temperature and the crystallization temperature with the size of the fractured specimens decreased was detected (the arrow in Fig. 5(a)). The decrease in the crystallization temperature indicates the decrease of the stability of the amorphous structure against crystallization. That is to say, the mobility and diffusibility of the atoms may be increased.

The plasticity of BMGs is usually studied in the framework of free volume model [25]. To investigate the possible change of free volume with specimen size, structural relaxation of the fractured specimens was studied using the DSC for temperatures below the glass transition temperature (the inset of Fig. 5(a)). It was observed that the area of the broad exothermic peak before the glass transition temperature increases from 0.6 J/g to 3.2 J/g when the diameter of the fractured

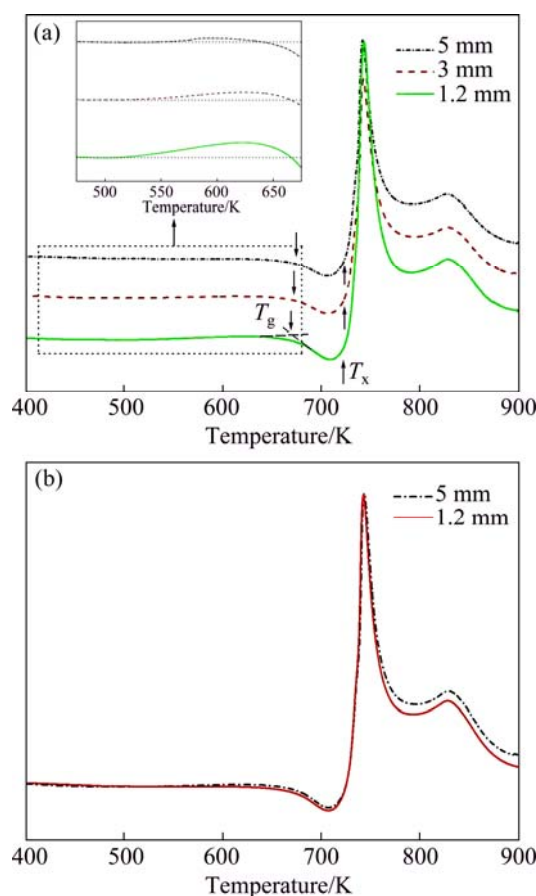


Fig. 5 DSC curves of glassy specimens with different diameters at heating rate of 20 K/min: (a) As-fractured; (b) Un-deformed

specimens decreases from 5 mm to 1.2 mm, as listed in Table 1. It is generally believed that prior to the glass transition temperature, an exothermic event is strongly linked with the existence of free volume in BMGs [26]. A model was proposed by BEUKEL and SEITSMA [26], in which the change in free volume is proportional to the variation of enthalpy during structural relaxation.

$$\Delta H_{fv} = \beta' \cdot \Delta v_f \quad (1)$$

where ΔH_{fv} is the change in enthalpy, β' is a constant, and Δv_f is the change of free volume per atomic volume. The value of ΔH_{sr} is shown in Table 1, suggesting that the smaller glassy specimen contains more free volume per atomic volume than the larger one after compression testing, presumably due to the deformation. On the contrary, this effect does not occur in the un-deformed specimens (Fig. 5(b)), indicating that there is no noticeable increase of free volume in small specimen after machining.

3.4 Hardness

Contrary to the cooling-rate induced hardening observed in crystalline metals, metallic glasses exhibit an entirely different behavior, i.e. cooling-rate induced

softening [18,19]. Figure 6(a) shows the Vickers hardness profile of the as-cast BMG sample with a diameter of 5 mm. It is clearly seen that the hardness is lower near the surface and increases steadily to a depth of $\sim 700 \mu\text{m}$, beyond which it remains roughly constant, similar to those reported in Ref. [18]. In contrast, for the as-machined specimens, the hardness profiles exhibit a relatively flat tendency and little change from the surface to the interior, as shown in Figs. 6(b) and (c).

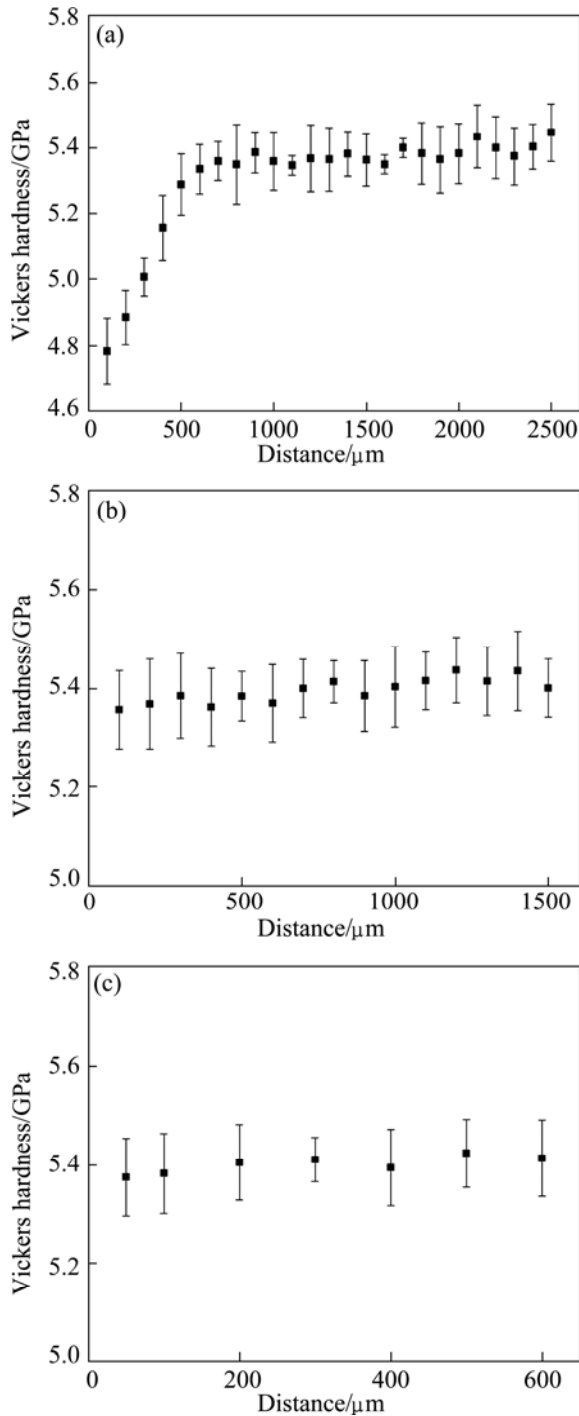


Fig. 6 Hardness profiles of 5 mm as-cast (a), 3 mm (b) and 1.2 mm (c) as-machined specimens (Error bars signify standard deviations from five measurements)

3.5 Fractograph

Examination of the fracture surface provided more information for further understanding the fracture mechanisms during the compressive deformation. Figure 7 shows the morphologies of fracture surface of 5 mm tested specimen. The fracture surface can be approximately divided into three regions. A comparatively smooth region A is present at the edge of the fracture surface, while region B exhibits less and thinner vein-like patterns than region C. The morphologies of fracture surface of 1.2 mm specimen after compression testing are shown in Fig. 8. Dense and multiple shear bands are found on the side surface (Fig. 8(a)), whilst plastic flow can be detected in some local regions on the fracture surface (Fig. 8(b)). In contrast to the large specimen, the small specimen shows a relatively smooth wrinkle-like fracture surface

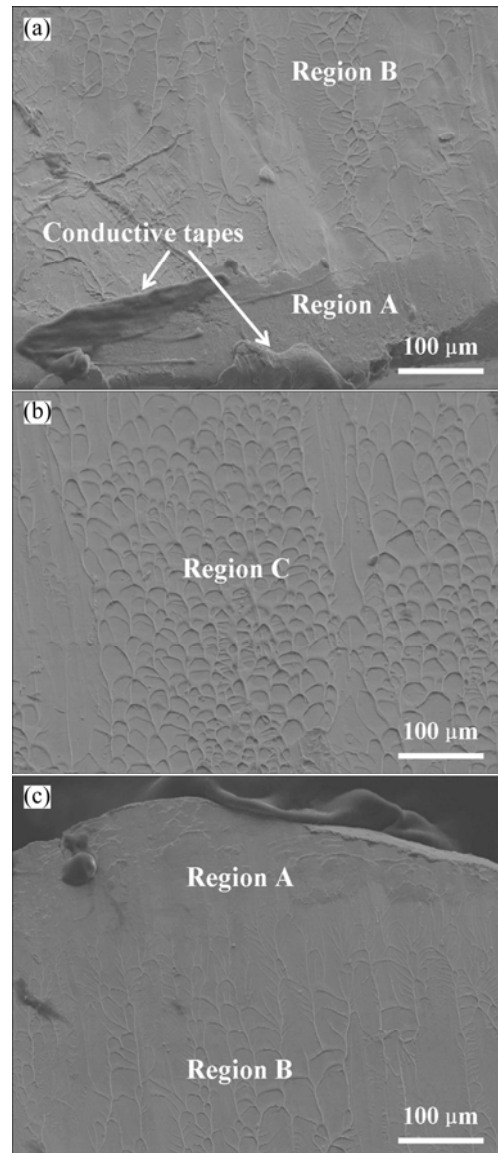


Fig. 7 Morphologies of fracture surface of 5 mm specimen: (a) Upper edge; (b) In center; (c) Lower edge

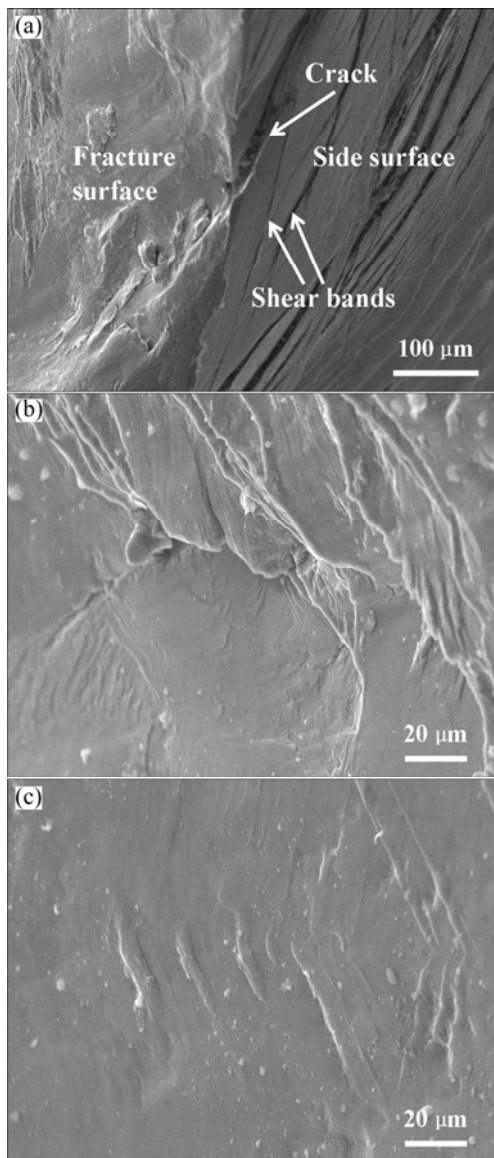


Fig. 8 Morphologies of fracture surface of 1.2 mm specimen: (a) Boundary of side surface and fracture surface; (b) Plastic flow; (c) Smooth surface

(Fig. 8(c)), which is consistent with the observations of XIE and GEORGE [24].

4 Discussion

Recently, the size effect on the mechanical behaviors of metallic glasses is widely studied [17,27, 28]. Nonetheless, owing to the absence of dislocations in metallic glasses, the real nature of the size effect on their mechanical behaviors is still controversial. Some reports proposed that the enhanced plasticity is attributed to the fact that specimen dimension decreased to the typical length-scale for the nucleation and propagation of shear bands [27]. In contrast, some results show that there is no appreciable size effect, even with specimen sizes ranged

from submicron to several millimeters [28]. In the present study, the specimens exhibit a seemingly evident size-dependant mechanical behavior. However, the underlying mechanism is completely different. First, the size difference in this work is not significant. Second, the size of the specimen is in millimeter level, which is large enough for the nucleation and propagation of shear bands. Third, the mechanical behaviors are actually derived from different parts of an identical specimen.

Since the cooling rate near the surface is higher than that inside the as-cast BMG, local atomic configurations could be different, even though they all have amorphous structure. LIU et al [18,19] studied the surface softening phenomenon induced by the cooling rate differences during casting in different metallic glasses, and deduced a correlation between cooling rate and defect concentration for further understanding the underlying mechanisms expressed as follows:

$$c_f = \frac{K}{(T - T_0)^2} \frac{dT}{dt} \quad (2)$$

where c_f is the defect concentration and is defined as the fraction of potential jumping sites of an atom, T_0 is the temperature at which the free volume disappears, K is a constant and (dT/dt) is the cooling rate. According to Eq. (2), the defect concentration is expected to be enhanced with the increase of the cooling rate. Higher defect concentrations offer more potential sites for atom jumping, thus increasing the mobility of atoms and decreasing the flow stress (hardness) [20]. Since the cooling rate was higher on surface than inside of the BMG during solidification, the amount of free volume in the near-surface region was larger than that at the center. This led to the smaller hardness in the surface layer than the interior (Fig. 6(a)).

The microstructure of the surface layer plays a significant role in the mechanical behavior of BMGs. For instance, ZHANG et al [9] characterized a softened surface layer in a shot-peened BMG and found that the softened layer induced by residual stress was of great benefit to improve the mechanical performance, particularly the compressive plasticity. However, the softened surface layer in the as-cast BMG was formed by the cooling-rate difference between the surface and the interior, which had no pre-existing shear bands, and the effect of any possible surface flaws introduced by polishing can also be ruled out. Further, BAKKAL et al [29] examined the surface microstructure of the same composition of BMG after machining at three different cutting speeds and revealed that there were no detectable crystallization occurring. This is in accordance with the present study (Fig. 1), implying that the potential effect of the crystalline phases produced by machining could be neglected.

In the as-cast large sample, the catastrophic crack initiated from the highly strained shear band and propagated rapidly from the soft surface to the hard inside. High defect concentrations generated by the high cooling rate in the near-surface region corresponded to a relatively loose atomic arrangement, which provided more favorable sites for atom jumping and moving, thus showing a low crack resistance under critical shear stress (low hardness). This led to rapid crack initiation and propagation along the most extremely deformed shear band, and the appearance of the comparatively smooth region (region A in Figs. 7(a) and (c)). With the development of the shear bands from the surface to the interior of the specimen, the local atomic arrangement became dense due to its low defect concentrations, and can hardly accommodate atom jumping. Accordingly, the propagation of shear bands was slowed down, while the dominant shear band was torn. These gave rise to the presence of typical vein-like patterns on the fracture surface (region C in Fig. 7(b)).

In the small specimen, considering the increase of free volume after compression testing, it is generally believed that strain softening occurred during the deformation. Strain softening induced by deformation processes, e.g., compression, milling, rolling, has been reported recently in different metallic glasses [30]. The free volume generated during deformation led to an increase in the diffusion of the atoms, and provided more favored sites for the nucleation of shear bands. Thus, more energy was stored in the smaller fractured specimen during deformation, perhaps as strain-induced local dilatation as well as an increase in interatomic distances. The latter could nucleate more shear bands, relieve the strain localization, and dissipate more loading energy, leading to the improvement of the plasticity [20]. In addition, more free volume in the small specimen could provide more potential sites for the motion and diffusion of the atoms on heating, which is in agreement with the decrease in the glass transition temperature and the crystallization temperature (see Fig. 5(a)).

It is worth noting that after compression test, the small specimen exhibits entirely distinct features on the fracture surface, indicating its particular fracture mechanism. XIE and GEORGE [24] suggested that the smooth surface was attributed to the stable shear band propagation. Unlike the large hardness discrepancy between the surface and the interior of the as-cast specimens (Fig. 6(a)), the as-machined samples have few variation of hardness due to the removal of the cast-softened surface, indicating more homogeneous microstructure and improved crack resistance. Consequently, the creation of shear-induced free volume in the glassy matrix, on one hand, can favor the nucleation of multiple shear bands on the surface,

alleviating the strain localization and dissipating more of the loading energy, hence giving rise to the enhancement of the plasticity; on the other hand, can promote more stable shear band propagation, leading to the presence of the relatively smooth wrinkle-like bands fracture surface (Fig. 8(c)). Moreover, the vein-like fracture surface is commonly thought to be a characteristic of reduced viscosity in shear bands, caused by the conversion of the stored elastic strain energy to heat. In contrast to the occurrence of high heating in a few highly localized shear bands of the large specimen, much less strain was applied in each shear band of the small specimen because of the multiplication of the shear bands. Therefore, the high strain was distributed, thus, resulted in relatively low heating, leaving smooth fracture surface.

5 Conclusions

1) The as-machined small specimens without the cast-softened layer exhibit highly dense and intersecting shear bands, and extensive plastic deformation, in contrast to the catastrophic failure and low deformability in the large specimens with the softened surface.

2) More free volume is detected in the small as-fractured specimens, indicating the occurrence of strain softening during the compressive process.

3) Compared with the relatively smooth fracture surface of the smaller specimens, the larger specimens show more diverse features on the fracture surface due to the graded structures.

References

- [1] GREER A L. Metallic glasses [J]. *Science*, 1995, 267: 1947–1953.
- [2] WANG W H, DONG C, SHEK C H. Bulk metallic glasses [J]. *Mater Sci Eng R*, 2004, 44: 45–89.
- [3] CHEN H, HE Y, SHIFLET G J, POON S J. Deformation-induced nanocrystal formation in shear bands of amorphous alloys [J]. *Nature*, 1994, 367: 541–543.
- [4] KHADEMIAN N, GHOLAMIPOUR R. Effects of infiltration parameters on mechanical and microstructural properties of tungsten wire reinforced $\text{Cu}_{47}\text{Ti}_{33}\text{Zr}_{11}\text{Ni}_6\text{Sn}_2\text{Si}_1$ metallic glass matrix composites [J]. *Transactions of Nonferrous Metals Society of China*, 2013, 23(5): 1314–1321.
- [5] LEE M L, LI Y, SCHUH C A. Effect of a controlled volume fraction of dendritic phases on tensile and compressive ductility in La-based metallic glass matrix composites [J]. *Acta Mater*, 2004, 52: 4121–4131.
- [6] KIM K B, DAS J, VENKATARAMAN S, YI S, ECKERT J. Work hardening ability of ductile $\text{Ti}_{45}\text{Cu}_{40}\text{Ni}_{7.5}\text{Zr}_5\text{Sn}_{2.5}$ and $\text{Cu}_{47.5}\text{Zr}_{47.5}\text{Al}_5$ bulk metallic glasses [J]. *Appl Phys Lett*, 2006, 89: 071908/1–071908/3.
- [7] CHEN L Y, FU Z D, ZHANG G Q, HAO X P, JIANG Q K, WANG X D, CAO Q P, FRANZ H, LIU Y G, XIE H S, ZHANG S L, WANG B Y, ZENG Y W, JIANG J Z. New class of plastic bulk metallic glass [J]. *Phys Rev Lett*, 2008, 100: 075501/1–075501/4.
- [8] SCHROERS J, JOHNSON W L. Ductile bulk metallic glass [J]. *Phys Rev Lett*, 2004, 93: 255506/1–255506/4.

- [9] ZHANG Y, WANG W H, GREER A L. Making metallic glasses plastic by control of residual stress [J]. *Nat Mater*, 2006, 5: 857–860.
- [10] LIN T, HU Y, KONG L, LI J. Effect of surface roughness on plasticity of $Zr_{52.5}Cu_{17.9}Ni_{14.6}Al_{10}Ti_5$ bulk metallic glass [J]. *Transactions of Nonferrous Metals Society of China*, 2012, 22(6): 1407–1411.
- [11] TIAN J W, SHAW L L, WANG Y D, YOKOYAMA Y, LIAW P K. A study on the surface severe plastic deformation behavior of a Zr-based bulk metallic glass (BMG) [J]. *Intermetallics*, 2009, 17: 951–957.
- [12] HUANG Y, SUN Y, SHEN J. Tuning the mechanical performance of a Ti-based bulk metallic glass by pre-deformation [J]. *Intermetallics*, 2010, 18: 2044–2050.
- [13] SHANMUGAM S, RAMISSETTI N K, MISRA R D K, MANNERING T, PANDA D, JANSTO S. Effect of cooling rate on the microstructure and mechanical properties of Nb-microalloyed steels [J]. *Mater Sci Eng A*, 2007, 460–461: 335–343.
- [14] ELMAJDOUBI M, VU-KHANH T. Effect of cooling rate on fracture behavior of polypropylene [J]. *Theor Appl Fract Mec*, 2003, 39: 117–126.
- [15] MOTEMANI Y, NILI-AHMADABADI M, TAN M J, BORNAPOUR M, RAYAGAN S. Effect of cooling rate on the phase transformation behavior and mechanical properties of Ni-rich NiTi shape memory alloy [J]. *J Alloys Compd*, 2009, 469: 164–168.
- [16] JIANG W H, LIU F X, WANG Y D, ZHANG H F, CHOO H, LIAW P K. Comparison of mechanical behavior between bulk and ribbon Cu-based metallic glasses [J]. *Mater Sci Eng A*, 2006, 430: 350–354.
- [17] HUANG Y J, SHEN J, SUN J F. Bulk metallic glasses: Smaller is softer [J]. *Appl Phys Lett*, 2007, 90: 081919/1–081919/3.
- [18] LIU Y, BEI H, LIU C T, GEORGE E P. Cooling-rate induced softening in a $Zr_{50}Cu_{50}$ bulk metallic glass [J]. *Appl Phys Lett*, 2007, 90: 071909/1–071909/3.
- [19] LIU Y, WU H, HE S W, LIU C T, HUANG B Y. Casting effect on softening of metallic glasses [J]. *J Alloys Compd*, 2009, 483: 82–85.
- [20] SPAEPEN F. A microscopic mechanism for steady state inhomogeneous flow in metallic glasses [J]. *Acta Metall*, 1977, 25: 407–415.
- [21] ARGON A S. Plastic deformation in metallic glasses [J]. *Acta Metall*, 1979, 27: 47–58.
- [22] LIU C T, HEATHERLY L, EASTON D S, CARMICHAEL C A, SCHNEIBEL J H, CHEN C H, WRIGHT J L, YOO M H, HORTON J A, INOUE A. Test environments and mechanical properties of Zr-base bulk amorphous alloys [J]. *Metall Mater Trans A*, 1998, 29: 1811–1820.
- [23] BEI H, XIE S, GEORGE E P. Softening caused by profuse shear banding in a bulk metallic glass [J]. *Phys Rev Lett*, 2006, 96: 105503/1–105503/4.
- [24] XIE S, GEORGE E P. Size-dependent plasticity and fracture of a metallic glass in compression [J]. *Intermetallics*, 2008, 16: 485–489.
- [25] JOHNSON W L, LU J, DEMETRIOU M D. Deformation and flow in bulk metallic glasses and deeply undercooled glass forming liquids—A self consistent dynamic free volume model [J]. *Intermetallics*, 2002, 10: 1039–1046.
- [26] van den BEUKEL A, SEITSMA J. The glass transition as a free volume related kinetic phenomenon [J]. *Acta Metall Mater*, 1990, 38: 383–389.
- [27] WU F F, ZHANG Z F, MAO S X. Size-dependent shear fracture and global tensile plasticity of metallic glasses [J]. *Acta Mater*, 2009, 57: 257–266.
- [28] SCHUSTER B E, WEI Q, HUFNAGEL T C, RAMESH K T. Size-independent strength and deformation mode in compression of a Pd-based metallic glass [J]. *Acta Mater*, 2008, 56: 5091–5100.
- [29] BAKKAL M, LIU C T, WATKINS T R, SCATTERGOOD R O, SHIH A J. Oxidation and crystallization of Zr-based bulk metallic glass due to machining [J]. *Intermetallics*, 2004, 12: 195–204.
- [30] JIANG W H, PINKERTON F E, ATZMON M. Mechanical behavior of shear bands and the effect of their relaxation in a rolled amorphous Al-based alloy [J]. *Acta Mater*, 2005, 53: 3469–3477.

铸造效应引发的块体非晶合金压缩脆性

吴宏^{1,2}, 刘咏¹, 李开洋¹, 赵中伟²

1. 中南大学 粉末冶金国家重点实验室, 长沙 410083;

2. 中南大学 冶金与环境学院, 长沙 410083

摘要: 研究 $Zr_{52.5}Cu_{17.9}Ni_{14.6}Al_{10}Ti_5$ 块体非晶合金由于铸造过程中表面与心部冷却速率差异诱发的表面软化层对其室温压缩行为的影响。通过逐层除去铸造表面软化层, 块体非晶试样表现出脆性–韧性转变。在室温压缩时, 除去表面软化层的试样呈现大量致密、均匀分布的剪切带和较好的塑性; 而未除去表面软化层的试样仅萌生出少量剪切带, 且发生灾难性断裂。除去软化层的试样变形后自由体积增加, 说明在压缩过程中发生了应变软化。除去软化层的试样组织结构相对均匀, 剪切带稳定扩展, 断面平滑; 而未除去表面软化层的试样则呈现出多样的断面形貌。

关键词: 块体非晶合金; 力学行为; 塑性变形; 剪切带; 自由体积

(Edited by Xiang-qun LI)